

# Journal of Materials Chemistry C

Accepted Manuscript



This is an *Accepted Manuscript*, which has been through the Royal Society of Chemistry peer review process and has been accepted for publication.

*Accepted Manuscripts* are published online shortly after acceptance, before technical editing, formatting and proof reading. Using this free service, authors can make their results available to the community, in citable form, before we publish the edited article. We will replace this *Accepted Manuscript* with the edited and formatted *Advance Article* as soon as it is available.

You can find more information about *Accepted Manuscripts* in the [Information for Authors](#).

Please note that technical editing may introduce minor changes to the text and/or graphics, which may alter content. The journal's standard [Terms & Conditions](#) and the [Ethical guidelines](#) still apply. In no event shall the Royal Society of Chemistry be held responsible for any errors or omissions in this *Accepted Manuscript* or any consequences arising from the use of any information it contains.

# A tetrathiafulvalene grafted titanium-oxo-cluster material: self-catalyzed crystal exfoliation and photocurrent responsive properties

Cite this: DOI: 10.1039/x0xx00000x

Received 00th January 2012,  
Accepted 00th January 2012

DOI: 10.1039/x0xx00000x

www.rsc.org/

Jing-Xue Yin,<sup>a</sup> Peng Huo,<sup>a</sup> Sheng Wang,<sup>a</sup> Jing Wu,<sup>a</sup> Qin-Yu Zhu<sup>\*a,b</sup> and Jie Dai<sup>\*a,b</sup>

Booming development has been achieved in exfoliation strategies for preparation of 2-D sheet materials from single crystals. However, most reported researches are concerned with crystals in micro scale. Bulky crystals turning to micro/nano structures are seldom achieved by chemical etching, because it is not easily completed for large crystals. We find a new material that can be exfoliated easily in millimeter crystal scale. The new material is a tetrathiafulvalene (TTF) grafted titanium oxo cluster (TOC), TiO-TTF. It is the first example that a TOC cluster is successfully combined with a TTF moiety. Red crystal of TiO-TTF cluster can turn to black 'crystal' in oxygen atmosphere, which is composed of regular arranged board-like micro plates. The good exfoliation property of the material arises from the easy oxidation property of the TTF group and catalytic property of the TiO cluster. The TTF moiety on cluster not only plays as the oxidation center, but also adds new photoelectroactive property to the TiO material. An enhanced photocurrent response is observed for the TiO-TTF and TiO-TTF(+) materials.

## 1. Introduction

Generalized concept of crystal engineering is a discipline to synthesize compounds or materials with targeted crystal structures, properties, or crystal morphologies. Crystal engineering in micro/nano scale involves mainly the crystal morphology control and morphology-property relationships, while in millimeter scale it involves mainly the molecular or ion assembly, structural analysis, and the structure-property relationships. Based on the CCDC data base,<sup>1</sup> since the later of the last century, about one million organic or organic-inorganic compounds have been structurally characterized by single crystal analysis using 0.1–1.0 mm scale single crystals. In contrast to the use in single crystal structure analysis, the study on the properties of millimeter scale single crystal material itself is limited. Recently, single crystal structure analysis has become a common technique, and organic or organic-inorganic scientists in this discipline now pay more attention to the properties and applications of the single crystal materials. Since the phenomena of single-crystal-to-single-crystal phase transitions were reported, the study on phase transitions of single crystals in millimeter scale has become a hotspot.<sup>2</sup> Researches on organic single crystal anisotropic conductors,<sup>3</sup> field-effect transistor,<sup>4</sup> single crystal photochemical device,<sup>5</sup> gas permeation and absorption, ion probing of bulky single crystals, and porous single crystals also become the interesting points.<sup>6</sup>

Along a different line of research, accompanying the booming development of 2-D graphene, more and more 2-D single crystal sheets of inorganic graphene analogues with atomic thickness have been fabricated from single crystals by exfoliation strategy.<sup>7</sup> However, most of the researches are on the micro/nano scale crystals. Bulky crystals turning to the micro/nano structures are seldom achieved except the thermodecomposition of the organic-metal crystals. In most cases the crystals are collapsed during the removing of the organic part. Recently, we found an interesting phenomenon: a TiO catalyzed redox exfoliation for bulky millimeter scale crystals. The original aim of the work is to study titanium-oxo-clusters (TOCs) functionalized with chromophore moieties, which is inspired by the applications of dye sensitized solar cells (DSCs).<sup>8</sup> The TOCs can be considered as the model compounds of the bulk nanoscale titanium oxides due to their perfectly defined structures for both experimental and theoretical studies.<sup>9</sup>

Tetrathiafulvalene (TTF, Chart 1) and its derivatives have attractive electron-donating and reversible redox properties. The design and synthesis of the TTF derivatives (TTFs) functionalized by various coordination groups along with the corresponding metal complexes have been extensively conducted during the past decade.<sup>10</sup> The TTF-metal complexes offer a novel perspective on multifunctional properties, for example, as the photoactive molecular materials.<sup>11</sup> Now, TTFs have been adsorbed on TiO films of photoactive systems and

applied in DSCs.<sup>12</sup> However, titanium-oxo-cluster grafted with TTF moiety has not even been explored. As the first compound that successfully combines the TOC with a tetrathiafulvalene ligand,  $[\text{Ti}_6\text{O}_3(\text{O}^i\text{Pr})_{14}(\text{L})_2] \cdot 0.5\text{H}_2\text{O}$  (TiO-L) ( $\text{HO}^i\text{Pr}$  = isopropanol,  $\text{L}$  = dimethylthio-tetrathiafulvalene dicarboxylate) is prepared and characterized by single crystal analysis. The TTF moiety of the cluster can be easily oxidized to a radical, giving an excellent photoelectroactive TiO material. More interestingly, the bulky single crystal can undergo self-catalytic oxidation and exfoliation to be a conductive material with stacks of micro plates. The work described here is also aimed at the fundamental studies of the TiO-TTF materials in photocurrent response.

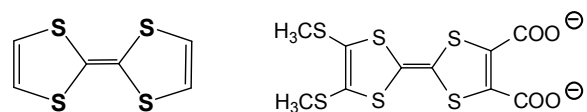


Chart 1. Structures of TTF (left) and L (right)

## 2. Results and discussion

### 2.1 Synthesis and crystal structure

Red crystals of cluster TiO-L are prepared directly by one step in situ solvothermal synthesis at 60 °C in isopropanol. The reaction between  $\text{Ti}(\text{O}^i\text{Pr})_4$  and  $\text{H}_2\text{L}$  follows the general scheme as reported for the analogue TiO-BDC (BDC = *o*-benzene dicarboxylate).<sup>10</sup> Detailed crystal data and structural refinement parameters for TiO-L are listed in Table S1. The experimental powder XRD pattern of the bulk microcrystal sample is in agreement with the simulated pattern from the crystal data of compound TiO-L (Figure S1). Thermogravimetry analysis (Figure S2) indicates that the compound gradually loses cocrystallized water molecule until 215 °C (3%) and a vigorous decomposition happens with the mass loss of 36% in the range of 215 to 248 °C, corresponding to the removal of the isopropanol, then in the range of 248 to 500 °C, the ligand decomposes. Finally, the  $\text{TiO}_2$  forms at the temperature about 800 °C (24%). Figure S3 shows the FTIR spectra of the red crystal TiO-L and the ligand  $\text{H}_2\text{L}$  for comparison. The stretches of the carboxyl group of TiO-L, 1604, 1561, and 1397  $\text{cm}^{-1}$ , indicate the coordination of the ligand L. Isopropoxy groups are detected by the  $\nu_{\text{C-H}}$  (2968 and 2924  $\text{cm}^{-1}$ ) and  $\nu_{\text{Ti-O-C}}$  (1009  $\text{cm}^{-1}$ ) vibrations.

Structural analysis shows that TiO-L crystallizes in  $P2_1/n$  space group and belongs to monoclinic system. The asymmetric unit includes two non-equivalent clusters and one cocrystallized water molecule. The structure of TiO-L shown in Figure 1a and Figure S4 contains two  $\text{Ti}_3\text{O}_{13}$  units which are linked together by one  $\mu_2$ -oxo atom and two L ligands via the  $\mu_2$ - $\eta^1$ : $\eta^1$  carboxylate chelate coordination bridges. Ball-stick plot of the  $\text{Ti}_3\text{O}_{13}$  unit is shown in Figure 1b, which is built by two  $\text{TiO}_6$  octahedra and one  $\text{TiO}_5$  trigonal bipyramid with co-shared edges (Figure 1a). The unique characteristic of TiO-L is the two coordinated wing-like TTF groups (Figure 1a and S5). A

number of similar titanium-oxo-clusters with two dual corner-missing cube subunits  $\text{Ti}_3\text{O}_3$  bridged by  $\mu_2$ -O or  $\mu_3$ -O have been reported,<sup>9a</sup> but only the structure of TiO-BDC<sup>13</sup> is the same as that of TiO-L. Figure 1c is the molecular packing showing the crystal angles.

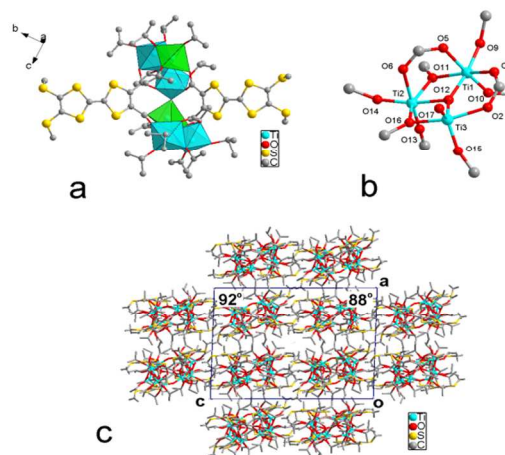


Figure 1. (a) Molecular structure of  $[\text{Ti}_6\text{O}_3(\text{L})_2(\text{O}^i\text{Pr})_{14}]$ . (b) Enlarged view of the  $\text{Ti}_3\text{O}_{13}$  cluster; isopropanol groups are omitted for clarity. (c) Molecular packing of TiO-L viewed along the *c* axis.

### 2.2 Optical and redox properties

Optical diffuse reflectance spectrum of the crystals of TiO-L was measured and the absorption data in the visible-near-IR range were calculated from the reflectance. The new absorption band, in comparison with that of TiO-BDC, is centered at 450 nm that is attributed to  $\pi$ - $\pi^*$  excitation of the TTF moiety (Figure S6). The energy band gap of TiO-L was estimated to be 2.1 eV from the UV-vis-NIR absorption band edge (585 nm), corresponding to the red color of the crystals. As usually observed in TTF derivatives (TTFs), two pairs of one-electron redox waves of TiO-L,  $E_{1/2}^1 = 0.463$  V (TTF<sup>•+</sup>/TTF) and  $E_{1/2}^2 = 0.792$  V (TTF<sup>2+</sup>/TTF<sup>•+</sup>), are observed by cyclic voltammetry (CV).<sup>10</sup>

To investigate the possibility of photoelectron transitions, a TDDFT calculation was performed on clusters TiO-L and TiO-BDC. The theoretical calculations of the excitation bands are in agreement with the experimental results of the spectra. For TiO-L cluster, the lowest energy transition is involved with the third excited state, including the transitions of HOMO-LUMO, HOMO-LUMO+1, and HOMO-LUMO+2 at 592 nm (2.3 eV) with an oscillator strength of 0.0102. The fourth excited state includes the transitions of HOMO-1-LUMO, HOMO-1-LUMO+1, and HOMO-1-LUMO+2 at 513 nm (2.4 eV) with an oscillator strength of 0.0309. The HOMO and LUMO of TiO-BDC have energies of -7.00 and -2.30 eV, respectively (Table S2), corresponding to a HOMO-LUMO gap ( $\Delta E = E_{\text{LUMO}} - E_{\text{HOMO}}$ ) of 4.70 eV. The HOMO and LUMO of TiO-L have

energies of  $-5.33$  and  $-2.53$  eV, respectively, in comparison with the TiO-BDC, the energy of HOMO increases and that of LUMO decreases. The energy of the HOMO–LUMO gap in the titanium clusters with L is smaller than that in TiO-BDC.

### 2.3 Self-catalyzed single crystal exfoliation

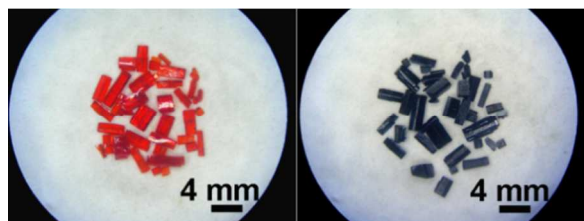


Figure 2. Photos of the red crystals of TiO-L and the blackened crystals.

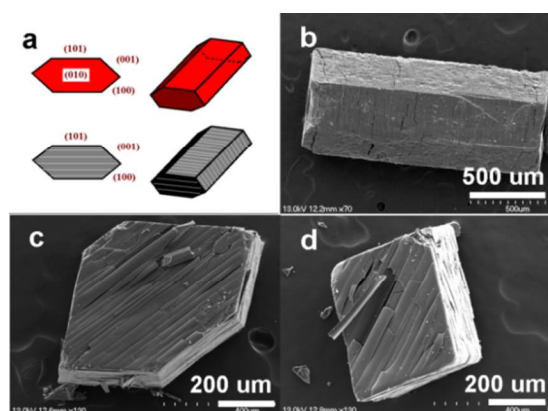


Figure 3. (a) Schematic drawing showing the crystal faces and the cracking texture of the single blackened crystal. SEM images of (b) a small crystal; (c) floor-board-like plates observed on (010) face; (d) disappearing of (101) face viewed along  $a$  axis.

It is very interesting that the red crystals of TiO-L cluster can turn to black gradually in ambient atmosphere and keep their crystal shape firmly (Figure 2). The crystal color changes quickly when they are exposed in oxygen atmosphere and that even happens in darkness. However, no color-change occurs if they are preserved in nitrogen atmosphere even for a long time, whatever with irradiation or non-irradiation. Therefore, the change should be an oxygen-involved oxidation process.

It is notable that after the change, the crystal of TiO-L cracks to a stacking with floor-board-like plates. Figure 3 shows the morphologies of the blackened crystal. Figure 3a is a schematic drawing showing the crystal faces and the cracking texture of the single crystal. Figure 3b shows the SEM image of a small blackened crystal. The (010) face is the most developed one, and the floor-board-like plates of the blackened crystal are observed on this face (Figure 3c). The (101) face disappears in some cases (Figure 3d). Figure S8 shows the layered structures on (101), (001) and (100) faces. Figure 4 shows the details of the plates. The surface of the plates is smooth and compact (Figure 4a and 4b), and the thickness of the plates is related to

the tendency of exfoliation. It is about 100–200 nm estimated from the side views of the layered structure (Figure 4c and 4d).

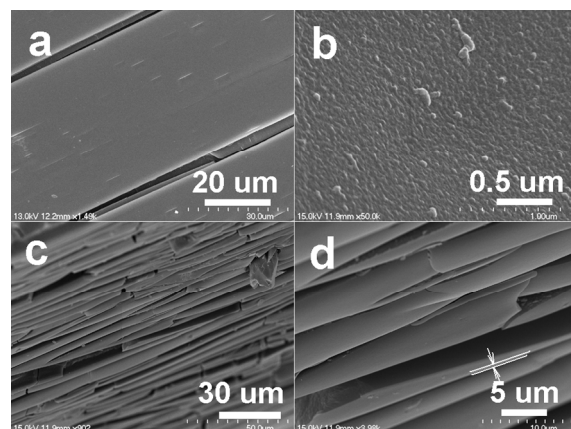


Figure 4. SEM images of the morphologies of the blackened crystal: (a, b) surfaces of the plates; (c, d) side views of the plates showing the layered structure.

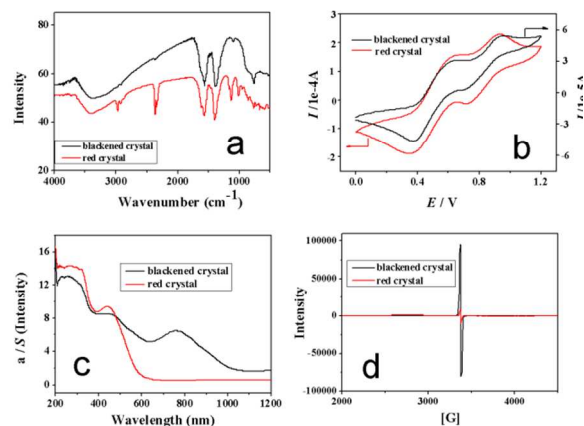
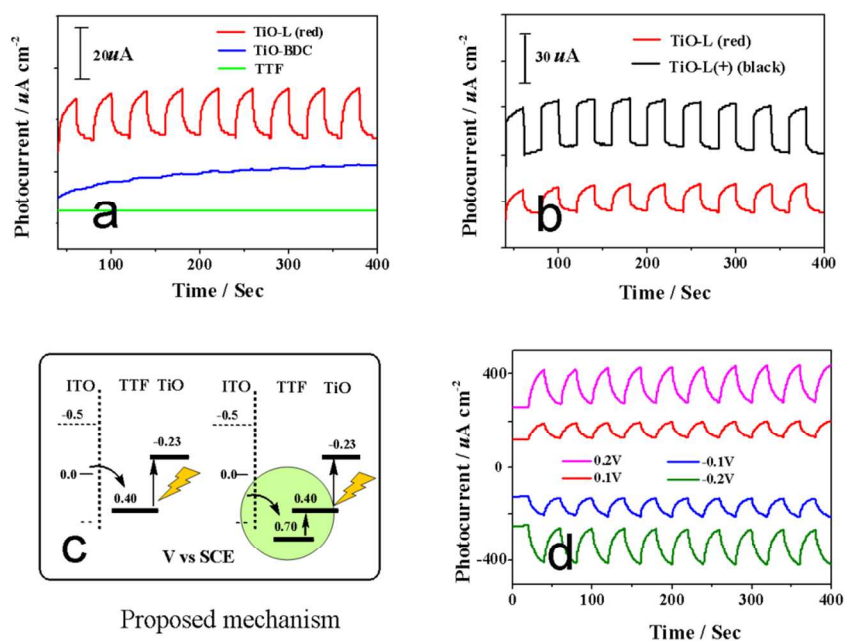


Figure 5. (a) FTIR spectra; (b) Solid state cyclic voltammogram in  $\text{CH}_3\text{CN}$  ( $0.1 \text{ mol}\cdot\text{L}^{-1} \text{ Bu}_4\text{NClO}_4$ ,  $100 \text{ mV s}^{-1}$ ); (c) UV-vis-NIR absorption spectra; (d) ESR spectra recorded at 110 K of the red crystals TiO-L and the blackened crystals.

The regular exfoliation or cracking of the crystal is fascinating to be further investigated. The black ‘crystals’ are characterized by various measurements. FTIR spectra (Figure 5a) show that there are no obvious changes for the bands of the blackened crystals in the range of  $1250$  to  $1750 \text{ cm}^{-1}$  in comparison with those of the red crystals TiO-L, indicating that the ligand L may be still coordinated to the TiO cluster. The  $\nu_{\text{C-H}}$  (about  $2900 \text{ cm}^{-1}$ ) and  $\nu_{\text{Ti-O-C}}$  (about  $1050 \text{ cm}^{-1}$ ) vibrations of the black ‘crystals’ are largely weakened, while the Ti-O-Ti vibration band at about  $750 \text{ cm}^{-1}$  is increased obviously, which shows that the isopropoxy groups in the red crystals are lost during the oxidation process and cluster to cluster condensation occurs. Solid state cyclic voltammogram confirms the reservation of the TTF moiety, because the characteristic signal of TTF, two pairs of redox waves, appears clearly (Figure 5b). The solid-state absorption spectrum of the black ‘crystals’ shows a new broad and intense band in the visible-near-IR

range with a maximum located at about 760 nm (Figure 5c) that is close to those reported for the one electron oxidized TTF compounds, in which an intense band of TTF radical cation appears in the range 700–800 nm.<sup>14</sup> The formation of the TTF radical cation is further supported by EPR study on this sample, which shows a very intense signal characteristic of a TTF radical cation ( $g = 2.008$ , Figure 5d). Based on the fact that the CV potentials of TiO-L are similar to those of the TTF ligand H<sub>2</sub>L (Figure S7) which is stable in oxygen, the phenomenon that the TiO-L is easy to be oxidized and exfoliated should be attributed to the catalyzed action of the TiO cluster on TTF oxidation in the presence of O<sub>2</sub> and self-condensation of TiO clusters. With all the information, the blackened crystal should be a TTF radical cation coordinated polymeric TiO product. Assisted by elemental analyses (Experimental section), the formula of the black 'crystal' should be [Ti<sub>6</sub>O<sub>11</sub>(L)<sub>2</sub>] $\cdot$ nH<sub>2</sub>O, TiO-L(+), in which every two isopropoxy groups of the TiO-L is replaced with a  $\mu_2$ -O atom due to the polymeric condensation. The cluster condensation and positive charged TTF radical play important roles in the exfoliation or cracking of the crystal, which happen directionally.

#### 2.4 Photocurrent response



**Figure 6.** Photocurrent responses in the presence of a 0.1 mol·L<sup>-1</sup> Na<sub>2</sub>SO<sub>4</sub> aqueous solution with -0.5 V applied potential of (a) TiO-L, TiO-BDC, TTF and (b) TiO-L and TiO-L(+). (c) Proposed mechanism of the photocurrent responses of TiO-L (left) and TiO-L(+) (right). (d) Photocurrent responses of black crystal TiO-L(+) measured as Schottky-type devices at different bias potentials.

The black line in Figure 6b shows the photocurrent responses of the black crystals, TiO-L(+), also measured under the same experimental conditions. The photocurrent of TiO-L(+) is about 30 μA·cm<sup>-2</sup>, about two times increase in comparison with that of TiO-L. Furthermore, the photoresponse of TiO-L(+) is faster than that of TiO-L. The photocurrent of

Although TiO clusters have been investigated as precursors for photoactive material<sup>16</sup> and TTF derivatives have been found photoelectroactive,<sup>11</sup> the researches on photoelectric transition of TiO-TTF system were scarce. In the limited examples, TTFs are adsorbed on the TiO films and their structural details are unclear.<sup>12</sup> The property of TiO cluster-TTF system has not been explored and the TTF radical modified TiO photoelectroactive system is still unknown to the best of our knowledge.

To investigate the effect of TTF on photocurrent response of the TiO cluster, cluster TiO-L coated ITO plate is used as a working electrode in a photoelectrochemical cell for measurement (see experimental section). Upon repetitive irradiation with xenon light on and off (interval 20 seconds), a clear photocurrent response is observed with -0.5 V applied potential (Figure 6a, 16 μA cm<sup>-2</sup>, red line). The repeatable cathodic photocurrents of TiO-L indicate the cooperative effect of TTF on the photocurrent generation of TiO cluster, because the TiO-BDC electrode displays very weak photocurrent response (blue line) and the TTF itself (green line) displays no observable light-gated response in μA scale under the same experimental conditions.

TiO-L(+) reaches the saturated state immediately (0.2 seconds), while the photoresponse time of TiO-L is about 5 seconds (turning to the platform). A two-probe method was used to measure the conductivities of the TiO-L and TiO-L(+) samples. The results show that TiO-L(+) possesses semiconductive property ( $6.89 \times 10^{-4}$  S·cm), while the TiO-L are nonconductors. The higher current intensity and the faster

response time (higher carrier mobility) confirm the positive effect of TTF(+) on the photocurrent generation of TiO cluster. The result has been verified by repetitive experiments and this finding is significant for developing new photoelectroactive systems.

Proposed mechanism of the photocurrent responses is described in Figure 6c. The energy of anatase is used as that of the conduction band edge of the polymerized TiO cluster and converted vs. SCE (-0.23 V).<sup>17</sup> The one electron redox potentials of TTF moiety of TiO-L and TTF(+) moiety of TiO-L(+) are about 0.4 and 0.7 V, respectively, which are estimated from the CV waves. The TTF moiety is an electron donor and the TiO cluster is an electron acceptor due to the high valence of Ti(IV). The electron transfer from TTF to TiO cluster is photoactivated and then the generated TTF(+) radicals obtain electrons from the electrode (Figure 6c, left). Because both the TiO-L(+) and TiO-L systems exhibit the same cathodic photocurrents, the mechanism of the two systems should be similar. Under the applied negative potential (-0.5 V), the TiO-L(+) is easy to be partially reduced and then the neutral TiO-L is photo-excited (Figure 6c, right). The conductive TiO-L(+) material, or more exactly the TiO-L(+)/TiO-L mixed state material, has higher carrier mobility, so that they show higher current response in comparison with that of the neutral one.

A simple Schottky-type device is also used to detect the photocurrent response property of the two materials. The electroactive layer is sandwiched between two electrodes. The thickness of the active layer is about 100  $\mu\text{m}$ . A potential is applied on the device, which facilitates the extraction of charge carriers. Figure 6d shows the photocurrent response of the blackened TiO-L, namely TiO-L(+), sandwiched between two ITO electrodes with applied potentials of -0.2, -0.1, 0.1, and 0.2 V. Steady photoresponses in current upon irradiation are observed. The intensity and current direction are directly related to the applied potentials. No such photocurrent response is detected for TiO-BDC and TiO-L in  $\mu\text{A}$  scale. These results indicate that the TiO-L(+) is an excellent photoelectroactive new material.

### 3. Conclusions

In summary, we successfully combine TOC with TTF dicarboxylate in a unique structure and the TiO-L cluster is first prepared and characterized by single crystal analysis. Interestingly, the red crystal of cluster TiO-L can turn to black 'crystal' in oxygen atmosphere, which is composed of regular arranged board-like micro plates. The good exfoliation property of the material arises from the easy oxidation property of the TTF group and catalytic property of the TiO cluster. TiO-L exhibits an effective photocurrent response and the TiO-L(+) is a more excellent photoelectroactive material due to the effect of the radical property of the oxidized TTF moiety. The controllable self-catalyzed exfoliation of TiO-L cluster and favorable photocurrent response of TiO-L(+) will encourage us to further challenge such materials.

## 4. Experimental

### 4.1 General Remarks

The compound, dimethyl tetrathiafulvalene dicarboxylate acid, was prepared using the method reported previously.<sup>18</sup> All analytically pure reagents were purchased commercially and used without further purification. Elemental analyses of C, H, and S were performed using a vario MICRO cube elemental analyzer. The FT-IR spectra were recorded as KBr pellets on a Nicolet Magna 550 FT-IR spectrometer. Solid-state room-temperature optical diffuse reflectance spectra of the compounds were obtained with a Shimadzu UV-3150 spectrometer. Cyclic voltammetry (CV) experiments were performed on a CHI650 electrochemistry workstation in a three-electrode system, a crystal coated ITO plate working electrode, a Pt wire auxiliary electrode, a saturated calomel electrode (SCE) as a reference electrode, and 0.1 mol·L<sup>-1</sup> Bu<sub>4</sub>NClO<sub>4</sub> as the supporting electrolyte. Solid-state EPR spectra were recorded by an EMX-10/12 spectrometer with a 100 kHz magnetic field in X band at 110K. PXRD of micro crystal samples were carried out on D/MAX-3C X-ray diffraction meter with Cu K $\alpha$  ( $\lambda = 1.5406 \text{ \AA}$ ) radiation. Thermal analysis was conducted on a TGA-DCS 6300 microanalyzer. The samples were heated under a nitrogen stream of 100 mL·min<sup>-1</sup> with a heating rate of 20 °C·min<sup>-1</sup>. The measurement of the morphology was carried out with a JSM-5600LV scanning electron microscope (SEM).

### 4.2 Preparation of Compounds

**[Ti<sub>6</sub>O<sub>3</sub>(L)<sub>2</sub>(O<sup>i</sup>Pr)<sub>14</sub>]·0.5H<sub>2</sub>O (TiO-L).** Analytically pure Ti(O<sup>i</sup>Pr)<sub>4</sub> (0.1 mL, 0.26 mmol) and H<sub>2</sub>L (7.6 mg, 0.020 mmol) are mixed in 0.2 mL anhydrous isopropanol and 0.2 mL acetone. The mixture is placed in a thick Pyrex tube (0.7 cm dia., 15 cm length) and quickly degassed by argon. The sealed tube is heated under autogenous pressure at 60 °C for 4 days, and then cooled to room temperature to yield red brick crystals (10 mg, 51.6 % yield based on L). The crystals are rinsed with isopropanol, and dried. The compound is preserved under sealed and dry nitrogen. Anal. Calcd for C<sub>124</sub>H<sub>222</sub>O<sub>51</sub>S<sub>24</sub>Ti<sub>12</sub> (MW 3873.02): C, 38.45; H, 5.78; S, 19.87. Found: C, 38.49; H, 5.65; S, 19.90. Important IR data (KBr, cm<sup>-1</sup>): 2968(w), 2924(w), 1604(m), 1561(m), 1397(m), 1122(m), 1009(m), 762(vw).

**[Ti<sub>6</sub>O<sub>3</sub>(BDC)<sub>2</sub>(O<sup>i</sup>Pr)<sub>14</sub>] (TiO-BDC)** (BDC = *o*-benzene dicarboxylate). The compound TiO-BDC is prepared according to the method reported previously.<sup>13</sup>

**[Ti<sub>6</sub>O<sub>11</sub>(L)<sub>2</sub>]·nH<sub>2</sub>O (n ≈ 13) [TiO-L(+)].** Red crystals of [Ti<sub>6</sub>O<sub>3</sub>(L)<sub>2</sub>(O<sup>i</sup>Pr)<sub>14</sub>]·0.5H<sub>2</sub>O are placed in a glass tube, filled with oxygen and then laid for 6 hours. Black crystal-shaped product is obtained and then dried in vacuum. Anal. Calcd for C<sub>20</sub>H<sub>38</sub>O<sub>32</sub>S<sub>12</sub>Ti<sub>6</sub> (MW 1462.5): C 16.43; H 2.62; S 26.31. Found: C 16.29; H 2.32; S 26.03. Important IR data (KBr, cm<sup>-1</sup>): 2916(vw), 1608(m), 1567(m), 1385(m), 1091(vw), 780 (broad), 762(w).

TiO-L(+) can also be obtained by exposing TiO-L in ambient atmosphere for 3 days.

### 4.3 X-ray crystallographic study

The measurement was carried out on a Rigaku Mercury CCD diffractometer with graphite monochromated Mo K $\alpha$  ( $\lambda = 0.71075$  Å) radiation. The X-ray crystallographic data were collected and processed using CrystalClear (Rigaku).<sup>19</sup> The structure was solved by direct methods using SHELXS-97, and refinement against all reflections of the compound was performed using SHELXL-97.<sup>20</sup> All non-hydrogen atoms were refined anisotropically. Hydrogen atoms of the methylthio groups were positioned with idealized geometry and refined with fixed isotropic displacement parameters. Hydrogen atoms of the O<sup>i</sup>Pr groups were not dealt with. CCDC 1019488 contains the supplementary crystallographic data for this paper. The data can be obtained free of charge from The Cambridge Crystallographic Data Centre via [www.ccdc.cam.ac.uk/data\\_request/cif](http://www.ccdc.cam.ac.uk/data_request/cif).

### 4.4 Electrode Preparation and Photocurrent Measurement

The photoelectrodes of the compounds were prepared by powder coating method. As a typical procedure, the crystals (0.003 mmol) were ground and pressed uniformly on the cleaned ITO glass (100  $\Omega/\square$ ). A 150 W high-pressure xenon lamp, located 20 cm away from the surface of the ITO electrode, was employed as a full-wavelength light source. The photocurrent experiments were performed on a CHI650E electrochemistry workstation in a three-electrode system, with the sample coated ITO glass as the working electrode mounted on the window with an area of 0.385 cm<sup>2</sup> ( $\Phi = 0.7$  cm), a Pt plate as auxiliary electrode and a saturated calomel electrode (SCE) as reference electrode. The supporting electrolyte solution was a 0.1 mol·L<sup>-1</sup> sodium sulfate aqueous solution. The lamp was kept on continuously, and a manual shutter was used to block exposure of the sample to the light.

A Schottky-type device was assembled to detect the photocurrent response property of the materials. The electroactive layer is sandwiched between two ITO electrodes. The thickness of the active layer is about 100  $\mu\text{m}$  and the effective irradiated area is 0.385 cm<sup>2</sup> ( $\Phi = 0.7$  cm). A proper potential was added on the device.

### 4.5 Theoretical Calculations

Density functional theory (DFT) calculations were carried out using GAUSSIAN 03 program package at the B3LYP level. The basis set used for C, O, S, and H atoms was 6-31G while effective core potentials with a LanL2DZ basis set was employed for Ti atom. The crystal structures of TiO-L and TiO-BDC were used as the initial structures and optimized to the minimum energy configurations. Throughout the calculations, OPri groups were replaced by OH groups in order to cut the computational cost with no significant change in the electronic properties. The theoretical and experimental bond lengths agree

within  $\sim 0.05$  Å (Table S3). Calculated electronic densities for the frontier orbitals of TiO-L and TiO-BDC are shown in Figure S9.

### Acknowledgements

We gratefully acknowledge financial support by the NSF of China (21171127 and 21371125), the Education Committee of Jiangsu Province (12KJB150020), the Priority Academic Program Development of Jiangsu Higher Education Institutions, and the Program of Innovative Research Team of Soochow University.

### Notes and references

- <sup>a</sup> College of Chemistry, Chemical Engineering and Materials Science, Soochow University, Suzhou 215123, P. R. China. Fax: +86 512 65880327; Tel: +86 512 6588 0327; E-mail: zhuqinyu@suda.edu.cn (Q.-Y. Zhu); daijie@suda.edu.cn (J. Dai)
- <sup>b</sup> State Key Laboratory of Coordination Chemistry, Nanjing University, Nanjing 210093, P. R. China.
- † Electronic Supplementary Information (ESI) available: XRD, TG and DTG, FTIR, molecular structure, UV-vis, CV, and theoretical calculation. See DOI: 10.1039/b000000x/. Crystallographic data in CIF format contain the supplementary crystallographic data for this paper, CCDC 1019488.
- 1 CCDC: Cambridge Crystallographic Data Centre, [www.ccdc.cam.ac.uk](http://www.ccdc.cam.ac.uk).
  - 2 a) M. Kawano and M. Fujita, *Coord. Chem. Rev.*, 2007, **251**, 2592–2605; b) G. Liu, J. Liu, Y. Liu and X. Tao, *J. Am. Chem. Soc.*, 2014, **136**, 590–593; c) T. Seki, K. Sakurada and H. Ito, *Angew. Chem. Int. Ed.*, 2013, **52**, 12828–12832; d) I. Halasz, *Cryst. Growth Des.*, 2010, **10**, 2817–2823 and references therein.
  - 3 a) T. Devic, M. Evain, Y. Moëlo, E. Canadell, P. Auban-Senzier, M. Fourmigué and P. Batail, *J. Am. Chem. Soc.*, 2003, **125**, 3295–3301; b) T. Nakanishi, T. Kojima, K. Ohkubo, T. Hasobe, K. Nakayama and S. Fukuzumi, *Chem. Mater.*, 2008, **20**, 7492–7500; c) Y. Geng, R. Pfattner, A. Campos, J. Hauser, V. Laukhin, J. Puigdollers, J. Veciana, M. Mas-Torrent, C. Rovira, S. Decurtins and S.-X. Liu, *Chem. Eur. J.*, 2014, **20**, 7136–7143; d) F. Pop, P. Auban-Senzier, A. Frąckowiak, K. Ptaszyński, I. Olejniczak, J. D. Wallis, E. Canadell and N. Avarvari, *J. Am. Chem. Soc.*, 2013, **135**, 17176–17186; e) F. Pop, P. Auban-Senzier, E. Canadell, G. L. J. A. Rikken and N. Avarvari, *Nat. Commun.*, 2014, 5:3757, DOI: 10.1038/ncomms4757.
  - 4 a) H. Li, B. C. K. Tee, J. J. Cha, Y. Cui, J. W. Chung, S. Y. Lee and Z. Bao, *J. Am. Chem. Soc.*, 2012, **134**, 2760–2765; b) A. L. Briseno, S. C. B. Mannsfeld, M. M. Ling, S. Liu, R. J. Tseng, C. Reese, M. E. Roberts, Y. Yang, F. Wudl and Z. Bao, *Nature*, 2006, **444**, 913–917; c) E. Ahmed, A. L. Briseno, Y. Xia and S. A. Jenekhe, *J. Am. Chem. Soc.*, 2008, **130**, 1118–1119; d) A. S. Molinari, H. Alves, Z. Chen, A. Facchetti and A. F. Morpurgo, *J. Am. Chem. Soc.*, 2009, **131**, 2462–2463.
  - 5 a) A. G. Shtukenberg, Y. O. Punin, A. Gujral and B. Kahr, *Angew. Chem. Int. Ed.*, 2014, **53**, 672–699; b) N. K. Nath, L. Pejov, S. M. Nichols, C. Hu, N. Saleh, B. Kahr and P. Naumov, *J. Am. Chem. Soc.*, 2014, **136**, 2757–2766; c) T. Kim, L. Zhu, L. J. Mueller and C.

- J. Bardeen, *J. Am. Chem. Soc.*, 2014, **136**, 6617–6625; d) N. Tokunaga, Y. Fujiki, S. Shinkaiab and K. Sada, *Chem. Commun.*, 2006, 3617–3618.
- 6 a) S. Takamizawa, Y. Takasaki and R. Miyake, *J. Am. Chem. Soc.*, 2010, **132**, 2862–2863; b) X. Li, H. Xu, F. Kong and R. Wang, *Angew. Chem. Int. Ed.*, 2013, **52**, 13769–13773; c) S. So and P. Schmuki, *Angew. Chem. Int. Ed.*, 2013, **52**, 7933–7935.
- 7 a) X. Zhang and Y. Xie, *Chem. Soc. Rev.*, 2013, **42**, 8187–8199; b) J. H. Han, S. Lee and J. Cheon, *Chem. Soc. Rev.*, 2013, **42**, 2581–2591.
- 8 a) B. O'Regan and M. Grätzel, *Nature*, 1991, **353**, 737–740; b) M. Grätzel, *Nature*, 2001, **414**, 338–344; c) A. Hagfeldt and M. Grätzel, *Acc. Chem. Res.*, 2000, **33**, 269–277.
- 9 a) L. Rozes and C. Sanchez, *Chem. Soc. Rev.*, 2011, **40**, 1006–1030; b) J. B. Benedict, R. Freindorf, E. Trzop, J. Cogswell and P. Coppens, *J. Am. Chem. Soc.*, 2010, **132**, 13669–13671; c) J. D. Sokolow, E. Trzop, Y. Chen, J. Tang, L. J. Allen, R. H. Crabtree, J. B. Benedict and P. Coppens, *J. Am. Chem. Soc.*, 2012, **134**, 11695–11700; d) R. C. Snoberger, K. J. Young, J. Tang, L. J. Allen, H. H. Crabtree, G. W. Brudvig, P. Coppens, V. S. Batista and J. B. Benedict, *J. Am. Chem. Soc.*, 2012, **134**, 8911–8917.
- 10 a) M. B. Nielsen, C. Lomholt and J. Becher, *Chem. Soc. Rev.*, 2000, **29**, 153–164; b) J. L. Segura and N. Martín, *Angew. Chem. Int. Ed.*, 2001, **40**, 1372–1409; c) D. Canevet, M. Sallé, G. Zhang, D. Zhang and D. Zhu, *Chem. Commun.*, 2009, 2245–2269 and references therein; d) D. Lorcy, N. Bellec, M. Fourmigué and N. Avarvari, *Coord. Chem. Rev.*, 2009, **253**, 1398–1438; e) M. Shatruk and L. Ray, *Dalton Trans.*, 2010, **39**, 11105–11121; f) F. Gao, F.-F. Zhu, X.-Y. Wang, Y. Xu, X.-P. Wang and J.-L. Zuo, *Inorg. Chem.*, 2014, **53**, 5321–5327.
- 11 a) T. Kakinuma, H. Kojima, T. Kawamoto and T. Mori, *J. Mater. Chem. C*, 2013, **1**, 2900–2905; b) R. Pfattner, E. Pavlica, M. Jaggi, S.-X. Liu, S. Decurtins, G. Bratina, J. Veciana, M. Mas-Torrent and C. Rovira, *J. Mater. Chem. C*, 2013, **1**, 3985–3988. c) F. Pointillart, A. Bourdolle, T. Cauchy, O. Maury, Y. L. Gal, S. Golhen, O. Cadour and L. Ouahab, *Inorg. Chem.*, 2012, **51**, 978–984; d) F. Pointillart, B. L. Guennic, O. Maury, S. Golhen, O. Cadour and L. Ouahab, *Inorg. Chem.*, 2013, **52**, 1398–1408; e) Y.-G. Sun, S.-F. Ji, P. Huo, J.-X. Yin, Y.-D. Huang, Q.-Y. Zhu and J. Dai, *Inorg. Chem.*, 2014, **53**, 3078–3087.
- 12 a) S. Wenger, P.-A. Bouit, Q. Chen, J. Teuscher, D. D. Censo, R. Humphry-Baker, J.-E. Moser, J. L. Delgado, N. Martín, S. M. Zakeeruddin and M. Grätzel, *J. Am. Chem. Soc.*, 2010, **132**, 5164–5169; b) P.-A. Bouit, M. Marszalek, R. Humphry-Baker, R. Viruela, E. Ortí, S. M. Zakeeruddin, M. Grätzel, J. L. Delgado and N. Martín, *Chem. Eur. J.*, 2012, **18**, 11621–11629; c) Y. Geng, F. Pop, C. Yi, N. Avarvari, M. Grätzel, S. Decurtins and S.-X. Liu, *New J. Chem.*, 2014, **38**, 3269–3274; d) A. Amacher, C. Yi, J. Yang, M. P. Bircher, Y. Fu, M. Cascella, M. Grätzel, S. Decurtins and S.-X. Liu, *Chem. Commun.*, 2014, **50**, 6540–6542.
- 13 Y.-Y. Wu, W. Luo, Y.-H. Wang, Y.-Y. Pu, X. Zhang, L.-S. You, Q.-Y. Zhu and J. Dai, *Inorg. Chem.*, 2012, **51**, 8982–8988.
- 14 a) M. J. Frisch, et al., *Gaussian 03, Revision B.01*; Gaussian, Inc.: Pittsburgh, PA, 2003; b) A. D. Becke, *J. Chem. Phys.*, 1993, **98**, 5648–5652 and references therein. c) C. Lee, W. Yang and R. G. Parr, *Phys. Rev. B.*, 1988, **37**, 785–789.
- 15 a) R. Andreu, I. Malfant, P. G. Lacroix and P. Cassoux, *Eur. J. Org. Chem.*, 2000, 737–741; b) H. Xue, X.-J. Tang, L.-Z. Wu, L.-P. Zhang and C.-H. Tung, *J. Org. Chem.*, 2005, **70**, 9727–9734; c) Q.-Y. Zhu, Y. Liu, W. Lu, Y. Zhang, G.-Q. Bian, G.-Y. Niu and J. Dai, *Inorg. Chem.*, 2007, **46**, 10065–10070.
- 16 Y.-Y. Wu, P. Wang, Y.-H. Wang, J.-B. Jiang, G.-Q. Bian, Q.-Y. Zhu and J. Dai, *J. Mater. Chem. A*, 2013, **1**, 9862–9868.
- 17 a) M. Grätzel, *Acc. Chem. Res.*, 2009, **42**, 1788–1798; b) K. Hara, H. Sugihara, Y. Tachibana, A. Islam, M. Yanagida, K. Sayama and H. Arakawa, *Langmuir*, 2001, **17**, 5992–5999.
- 18 a) P. Hudhomme, S. L. Moustarder, C. Durand, N. Gallego-Planas, N. Mercier, P. Blanchard, E. Levillain, M. Allain, A. Gorgues and A. Riou, *Chem. Eur. J.*, 2001, **7**, 5070–5083; b) R. D. McCullough, M. A. Petruska and J. A. Belot, *Tetrahedron*, 1999, **55**, 9979–9998; c) P. Huo, J.-P. Wang, M.-Y. Shao, Y.-G. Sun, S.-F. Ji, Q.-Y. Zhu and J. Dai, *Phys. Chem. Chem. Phys.*, 2012, **14**, 16229–16235.
- 19 *CrystalClear*; Rigaku Corp.: 1999. *CrystalClear Software User's Guide*; Molecular Structure Corp.: 2000; J. W. Pflugrath, *Acta Crystallogr. Sect. D*, 1999, **55**, 1718–1725.
- 20 G. M. Sheldrick, *SHELXS-97, Program for structure solution*; Universität of Göttingen: Germany. 1999. G. M. Sheldrick, *SHELXL-97, Program for structure refinement*; Universität of Göttingen: Göttingen, Germany, 1997.

A unique TiO-TTF cluster is first reported. Its red single crystal undergoes self-catalytic oxidation-exfoliation to be black 'crystal' composed of regular arranged board-like microplates. It is characterized as the TTF radical modified TiO material. An enhanced photocurrent response is observed for the TiO-TTF radical materials.

